Desalination and Water Treatment
www.deswater.com

doi: 10.5004/dwt.2019.24561

167 (2019) 302–312
November

Electrochemical oxidation treatment of leather dyeing wastewater using response surface methodology

Kaouthar Oukili*, Mohammed Loukili

Laboratory of Process, Environment and Renewable Energy, Sidi Mohamed Ben Abdellah University, High School of Technology, BP 2427 Imouzzer Road, 30000 Fez, Morocco, Tel. +212650547553; email: kawtar.oukili91@gmail.com (K. Oukili), Tel. +212664061470; email: mohammed.loukili@usmba.ac.ma (M. Loukili)

Received 19 January 2019; Accepted 13 June 2019

ABSTRACT

The present study investigates the electrochemical oxidation (EO) of real leather dyeing wastewater coming from a local modern tannery in Fez (Morocco). Experiments were performed in an electrochemical reactor using Ti/Pt anode. Response surface methodology and full factorial central composite design were used to investigate the combined effect of three independent operating parameters considered for the optimization of the EO process: electrolysis time (t), current density (j) and temperature (T). Chemical oxygen demand (COD) removal (Y_1) and specific energy consumption (SEC) in kWh/kg of COD removed (Y_2) were used as responses to examine the degradation of wastewater. The obtained quadratic model was statistically tested using analysis of variance. The correlation coefficients for the model (R^2) were 0.9986 and 0.9830 for COD removal and SEC, respectively. The best conditions for maximum COD removal and minimum specific energy consumption in the present study were $t = 2.11$ h, $j = 18.70$ mA/cm^2 and $T = 286.18$ K. Under these optimum conditions, 81.2% of COD removal was observed with energy consumption of 93.85 kWh/kg of COD removal. Fourier transformed infrared spectroscopy analysis was used for the characterization of effluent. Evolution of inorganic ions concentration and changes of turbidity, pH and conductivity of wastewater during the EO process were also followed.

Keywords: Electrochemical oxidation; COD removal; Specific energy consumption; Response surface methodology; Leather dyeing wastewater

1. Introduction

The leather industry daily produces large amounts of wastewater highly polluted with toxic chemicals [1]. These effluents are deeply colored and contain high levels of refractory organic compounds and hazardous pollutants [2]. Therefore, the improper discharge of untreated tannery wastewater can cause severe environmental problems [3]. The dyeing step is carried out during the wet finishing process of leather production, and it requires a huge amount of water resources and chemicals [4], which highly increase the chemical oxygen demand (COD) of wastewater. Thus, it is necessary to apply effective treatment methods to deal with these organic pollutants prior to their discharge into receiving waters. Traditional biological treatment methods have demonstrated to be ineffective for the removal of these pollutants. In this context, several methods have been developed by researchers to improve the treatment efficiency of dye-containing wastewaters from tanneries [4,5]. Among the new technologies, electrochemical advanced oxidation processes (EAOP) such as electrochemical oxidation (EO) and electro-Fenton (EF) have received great attention for the degradation of recalcitrant organic compounds in recent years [6,7].

EO is one of the most promising EAOPs to treat such complex systems due to its ability to eliminate persistent

---

* Corresponding author.

hazardous contaminants efficiently without forming any kind of sludge. Many researchers have mentioned that EO can occur directly by direct charge transfer at the anode and indirectly by electrogenerated reactive oxygen species ($^{\bullet}$OH) radicals and/or active chlorine species (Cl_2, HOCl and ClO^-) [8]. The effectiveness of the EO process strongly depends on the anode material, and the operational conditions [2]. Several research groups have reported the effectiveness of EO using various electrode materials [9]. For instance, Tu et al. [10] studied the treatment of simulated berberine wastewater by EO with RuO_2/Ti, IrO_2/Ti, $RuIrO_2$/Ti and Pt/Ti electrodes. The results showed that Pt/Ti anode exhibited a higher removal rate of berberine than the other anodes. Metal oxide anodes have also attracted the attention of researchers. Rao and Venkatarangaiah [11] compared in their review paper the effectiveness of four metal oxide-coated anodes: SnO_2, PbO_2, IrO_2 and RuO_2, and they concluded that SnO_2 and PbO_2 anodes were suitable for the EO of wastewater treatment on large scale. Meanwhile, da Silva Duarte et al. [12] investigated the treatment of synthetic effluent containing rifampicin drug by applying EO with the combination of Fenton reaction. They compared the effect of different electrode materials and concluded the following order with respect to COD removal: BDD >> Ti/Pt > DSA.

For the EO treatment of dyes wastewater, Cotillas et al. [13] used boron-doped diamond (BDD) electrodes to oxidize Red MX-5B dye in aqueous solutions. After 240 min of EO, full dye and COD removal were achieved due to the high production of free-hydroxyl radicals, which attack the organic matter in the wastewater, promoting significant mineralization. Labiadh et al. [14] used different anodes (DSA, PbO_2 and BDD) to treat aqueous solutions containing methyl orange azo dye. The results showed that almost complete degradation was achieved using BDD and PbO_2 anodes after 3 h of EO, but BDD exhibited the better performance of COD removal, with 96% and 79% of mineralization, respectively. Conversely, on DSA electrode, 75% COD removal with 60% mineralization was obtained under similar experimental conditions. Isarain-Chávez et al. [15] examined the oxidation power of five different DSA anodes (Ti/Ir-Pb, Ti/Ir-Sn, Ti/Ru-Pb, Ti/Pt-Pd and Ti/RuO_2) for EO of methyl orange azo dye solutions. They reported complete removal of color in the case of Ti/Ir-Pb, Ti/Ir-Sn and Ti/Ru-Pb anodes, and lower decolorization in the case of Ti/Pt-Pd and Ti/RuO_2 anodes. Higher mineralization was achieved in 240 min (74%) using Ti/Ir-Pb anode. Kaur et al. [16] treated actual textile wastewater using RuO_2 coated Ti electrode (Ti/RuO_2) and they reported COD and color removals of 80% and 97%, respectively.

Despite the frequent use of EO for the degradation of synthetic or simulated textile dyes wastewaters [17], to our best knowledge, no studies have been devoted to the EO of leather dyeing wastewater, which is different from that of textile industry due to the presence of specific chemical compounds used in leather production. Furthermore, only a few papers are available in the literature about the electrochemical degradation of real dyeing wastewater [18–22] which is more complex compared with the synthetic effluent. Real dyeing wastewater contains mixtures of different types of dyes, as well as inorganic ions such as chloride, which can promote or inhibit the process. Therefore, performance and applicability of the EO process require more study on real effluents. In this context, the present study aims to evaluate the performance of the EO process with Ti/Pt electrodes and its applicability for the treatment of real leather dyeing wastewater. Effects of operating parameters such as electrolysis time (t), current density (j) and temperature (T) on COD removal (Y_1) and specific energy consumption (Y_2) were investigated. Central composite design (CCD) under response surface methodology (RSM) was employed in order to determine the optimal operating conditions that give high removal efficiency with low energy requirements. The characterization of leather dyeing wastewater by Fourier transformed infrared spectroscopy (FTIR) analysis was also studied. Furthermore, the evolution of inorganic ions concentration and changes of turbidity, pH and conductivity of wastewater during the EO process were also investigated.

2. Experimental

2.1. Tannery wastewater

The leather dyeing effluent (Table 1) used in the experiments was collected from a local modern tannery in Fez (Morocco). The wastewater was sedimented and filtered with soft paper prior to treatment. As mentioned in Table 1, the effluent has a high COD concentration, so dilution of raw wastewater before treatment becomes important to visualize better and clearer results. The effluent was diluted 10 times with distilled water.

2.2. Electrochemical experiments

Electrochemical experiments were performed using a cylindrical tank reactor of 6 L capacity, equipped with an external water-jacket to maintain the temperature at the desired setpoint using a thermostatic bath, ULTRATEMPS 2000 JULABO F30. The process was performed using Ti/Pt electrodes where the anode was a cylindrical grid with a large surface area of 600 cm^2, and the cathode was rod whose surface was 5% of that of the anode. The current was applied by a regulated DC power source, EA-7015-050. The solution was constantly stirred at 400 rpm to ensure homogeneity using a BIOBLOCK SCIENTIFIC stirrer.

2.3. Analytical methods

Performance of the process was evaluated by analyzing the COD removal efficiency and the specific energy consumption. The characterization of raw wastewater was done using FTIR analysis. COD (mg L^{-1} O_2) was measured using the closed-reflux colorimetric method with a Shimadzu/1201 spectrophotometer [23]. The efficiency of COD removal was calculated as follows (Eq. (1)):

$$\mathrm{COD}(\%) = \frac{\mathrm{COD}_i - \mathrm{COD}_t}{\mathrm{COD}_i} \times 100 \tag{1}$$

where COD_i and COD_t are chemical oxygen demands at times $t = 0$ (initial) and t, respectively.

The specific energy consumption (SEC), expressed in (kWh kg^{-1} COD) was calculated using Eq. (2).

Table 1
Characterization of raw and diluted wastewater

Parameters	Raw	Diluted
Color	Black	Black
pH	3.56	6.15
COD (mg L^{-1})	7,189	623
Turbidity (NTU)	11	26.3
TS (mg L^{-1})	330	–
Conductivity (mS/cm)	13.5	5.297
Nitrate (mg L^{-1})	0.742	0.081
Nitrite (mg L^{-1})	0.578	0.064

$$\text{SEC} = \frac{E_{\text{cell}} \times I \times \Delta t}{1000 \times V \times \Delta\text{COD}} \tag{2}$$

where E_{cell} is the applied voltage (V), Δt is the electrolysis time (h) and V is the reactor volume (L). The current efficiency (CE) for the EO of wastewater was calculated using Eq. (3).

$$\text{CE} = \frac{\left(\text{COD}_{t+\Delta t} - \text{COD}_{t}\right)\text{FV}}{8I\Delta t} \tag{3}$$

where COD_t and $\text{COD}_{\Delta t+t}$ are the COD values in (g O_2 L^{-1}) at time t and Δ_{t+t}, respectively, V is the volume of the electrolyte (L), I is the current (A) and F is the Faraday constant (96,487 C/mol). The inorganic ions (nitrate and nitrite) released during EO were examined according to the Standard Methods [24]. The pH and conductivity were detected with a HACH pH-meter (Model Sension 7) and a HACH conductivity meter. The turbidity of wastewater was measured by a TURBIDIRECT turbidimeter.

2.4. Experimental design and statistical analysis

In the present study, three important parameters such as electrolysis time (X_1), current density (X_2) and temperature (X_3) were selected to estimate the significance of the effects of these factors on two responses, that is, % COD removal and SEC using RSM with three-level CCD. The independent factors were coded as –1 (low), 0 (central point) and +1 (high). Also, α value of 1.68 was used to allow the prediction of the response functions outside the cubic domain [25]. Table 2 shows the range of each investigated variable and were t (min) = [2; 4], j (mA/cm²) = [8.3; 16.6], and T (K) = [293; 313].

The following second-order polynomial response equation was used to predict and describe the relationships between the COD removal and operational factors:

$$Y = b_0 + b_1X_1 + b_2X_2 + b_3X_3 + b_{12}X_1X_2 + b_{13}X_1X_3 + b_{23}X_2X_3 + b_{11}X_1^2 + b_{22}X_2^2 + b_{33}X_3^2 \tag{4}$$

where Y_1 and Y_2 are the responses studied, X_i and X_j are the independent variables, b_0 is constant coefficient, b_i, b_{ii} and b_{ij} are interaction coefficients of linear, quadratic and second-order terms, respectively. The significance and adequacy of the developed regression model were evaluated by the application of analysis of variance (ANOVA). The Minitab software (version 16.0) was used to analyze the experimental data.

Table 2
Levels of the parameters studied in CCD statistical experiment

	Coded variable				
Variable	−1.68	−1	0	+1	+1.68
Electrolysis time (h)	1.32	2	3	4	4.68
Current density (mA/cm²)	5.4	8.3	12.5	16.6	19.5
Temperature (K)	286.9	293	303	313	319.8

3. Results and discussion

3.1. Characterization of wastewater

Fig. 1 shows the FTIR spectra of the untreated wastewater. The intensive, broad bands in the range of 2,800–3,600 cm⁻¹ are associated with the stretching vibrations of –OH group, which indicates the presence of alcohols and carboxylic acid [26,27]. The peak at 3,432 cm⁻¹ for amide stretching (–N–H–) suggests the presence of primary and secondary amino groups (aliphatic or aromatic) [28]. Peaks at 2,923 and 2,853 cm⁻¹ occur due to aliphatic C–H groups [29,30]. The spectrum shows an obvious band at 1,634 cm⁻¹, which may be related to the stretching vibrations of alkene (–C=C–) group and bending vibrations of amide (–N–H–) bond [26,31]. The peak obtained at 1,732 cm⁻¹ was assigned to the carboxyl group (–C=O–) [32]. The stretching frequency at 1,383 cm⁻¹ may be related to the carboxyl–carbonate structures, stretching vibrations (–S=O–) of sulfate and the presence of aliphatic nitro (–NO_2) group [26,30]. The peaks in the range of 1,163; 1,115 and 1,031 cm⁻¹ are associated with the stretching vibrations of C–O ester group [33]. The peaks at 685.5, 777.1 and 526.8 cm⁻¹ indicate the aromaticity or benzene ring [34].

3.2. Model fitting and statistical analysis

The effects of operating variables of electrolysis time (t), current density (j) and temperature (T) on COD removal and SEC that were determined according to CCD and measured responses from 17 runs are demonstrated in Table 3. The COD removal and SEC in terms of coded variables have been expressed by the following quadratic Eqs. (5) and (6), respectively.

$$Y_1 = 59.61 + 8.49X_1 + 15.03X_2 - 4.3X_3 - 0.54X_1^2 - 1.41X_2^2 - 0.04X_3^2 + 1.99X_1X_2 - 0.31X_1X_3 + 0.006X_2X_3 \tag{5}$$

$$Y_2 = 122.38 + 17.53X_1 + 21.61X_2 + 5X_3 - 6.14X_1^2 - 3.09X_2^2 - 0.35X_3^2 + 4.84X_1X_2 - 0.55X_1X_3 - 0.86X_2X_3 \tag{6}$$

The statistical significance of the quadratic model was justified by the ANOVA using the Minitab software (Table 4). According to the results, the value obtained for the F-value

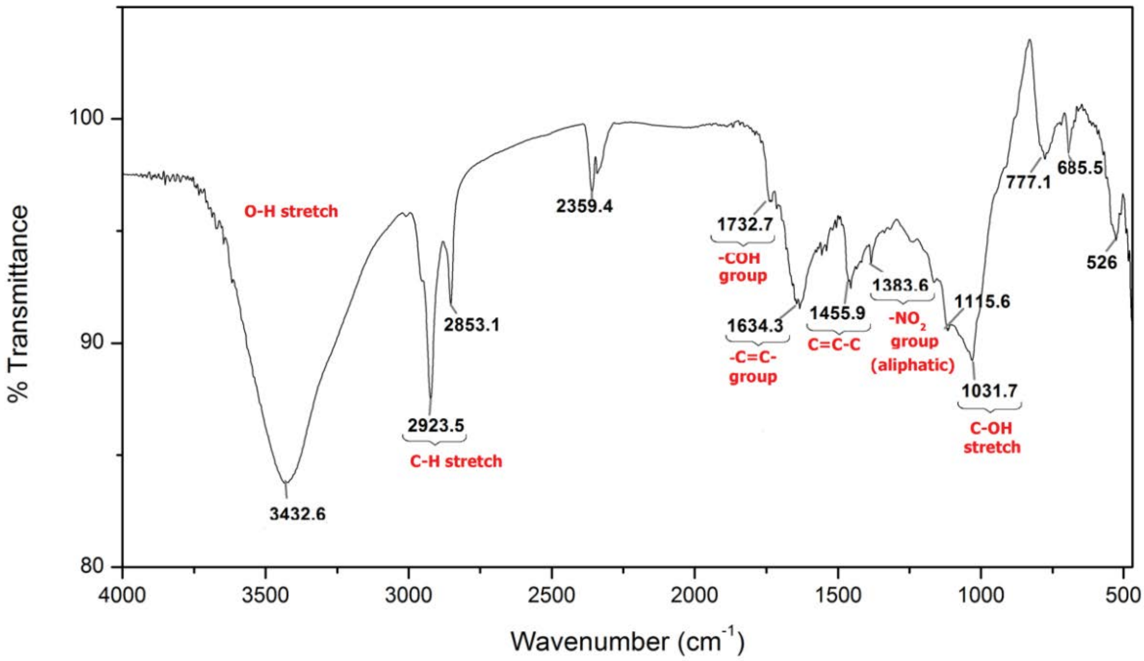

Fig. 1. FTIR of untreated wastewater.

Table 3
Central composite design matrix, responses results (% COD removal and SEC)

Run Number	Electrolysis time (h)	Current density (mA/cm^2)	Temperature (K)	% COD removal		SEC (kWh per kg COD removed)	
				Actual	Predicted	Actual	Predicted
1	−1 (2)	−11 (8.3)	−1 (293)	40.77	37.72	71.47	71.60
2	+1 (4)	−1 (8.3)	−1 (293)	52.42	54.70	101.49	105.80
3	−1 (2)	+1 (16.6)	−1 (293)	65.97	68.84	107.50	112.11
4	+1 (4)	+1 (16.6)	−1 (293)	86.91	85.82	152.91	146.31
5	−1 (2)	−1 (8.3)	+1 (313)	33.17	28.82	82.35	83.88
6	+1 (4)	−1 (8.3)	+1 (313)	44.89	45.80	106.17	118.08
7	−1 (2)	+1 (16.6)	+1 (313)	59.72	59.94	110.98	124.39
8	+1 (4)	+1 (16.6)	+1 (313)	78.09	76.92	158.09	158.59
9	−1.68 (1.3)	0 (12.5)	0 (303)	42.04	43.04	79.35	86.33
10	+1.68 (4.6)	0 (12.5)	0 (303)	73.71	71.60	134.71	143.85
11	0 (3)	−1.68 (5.4)	0 (303)	29.87	31.14	77.84	81.03
12	0 (3)	+1.68 (19.5))	0 (303)	80.94	83.49	153.46	149.15
13	0 (3)	0 (12.5)	−1.68 (286.9)	67.78	64.80	107.72	104.77
14	0 (3)	0 (12.5)	+1.68 (319.8)	50.80	49.83	139.07	125.42
15	0 (3)	0 (12.5)	0 (303)	60.06	57.32	121.12	115.09
16	0 (3)	0 (12.5)	0 (303)	59.86	57.32	121.59	115.09
17	0 (3)	0 (12.5)	0 (303)	58.98	57.32	123.74	115.09

parameter and very low *p*-value (<0.0001) confirm that the developed model was highly significant within a 95% confidence interval. Moreover, the fitness of the model was checked by the determination of coefficient (R^2). In the present case, the R^2 values for COD removal and SEC were close to 1 which indicates that the response surface quadratic model is a good option for predicting the performance of COD removal and SEC [35]. Furthermore, Fig. 2 shows a good agreement between the predicted and observed values. This indicated that the model was satisfactory and accurate [36].

Pareto analysis was also used to facilitate interpretation of the results. In fact, this analysis displays the effect of

Table 4
ANOVA results for % COD removal and SEC

Source	Df	SS	MS	F-ratio	p-value
		COD removal (%)			
Model	9	4,382.15	486.91	216.45	<0.0001
Residual	7	15.75	2.25		
Lack of fit	5	15.08	3.02	9.11	0.102
Total	16	8,021.64			
	RSME = 1.49 $R^2 = 0.9986$ $R^2_{\text{adj}} = 0.9968$ $R^2_{\text{Pre}} = 0.9733$				
		SEC			
Model	9	11,694.6	1,299.4	45.10	<0.0001
Residual	7	201.7	28.81		
Lack of fit	5	197.8	39.55		0.048
Total	16	11,896.2			
	RSME = 5.36 $R^2 = 0.9830$ $R^2_{\text{adj}} = 0.9612$ $R^2_{\text{Pre}} = 87.21$				

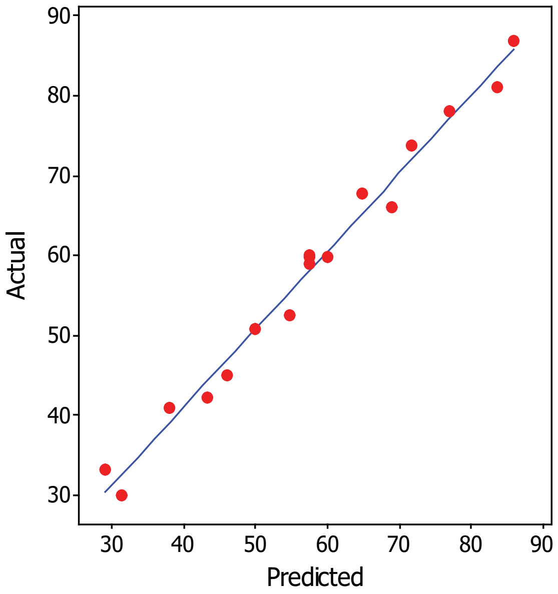

Fig. 2. Predicted vs. actual values of COD removal.

each factor on the response and was calculated based on the following equation [37,38]:

$$P_i = \frac{b_i^2}{\sum b_i^2} \times 100 \quad (i \neq 0) \tag{7}$$

where b represents the related regression coefficient of the parameter. According to the Pareto chart (Fig. 3), it can be seen that electrolysis time (22.32%) and temperature (5.72%) were statically significant whereas current density (69.98%) had the highest effect on COD removal efficiency by EO process. However, the quadratic term of current density (0.61%) and its interaction with electrolysis time (1.22%) were also considered significant while the other terms do not affect the process efficiency.

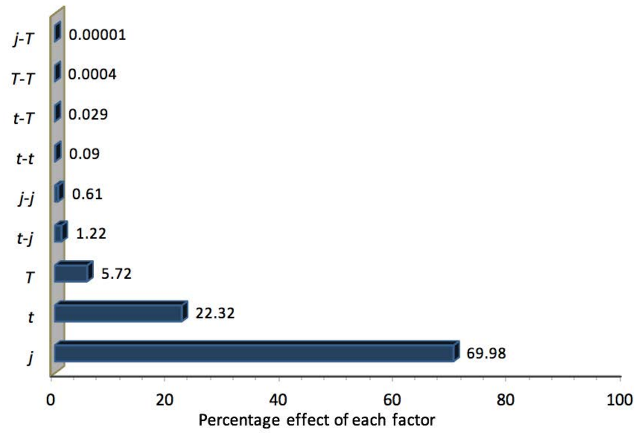

Fig. 3. Pareto graphic analysis.

3.3. Effect of parameters on responses

Based on Eqs. (6) and (7), the response surface graphs were developed and illustrated in Figs. 4a–d. As can be seen, j is the most important parameter for the removal of COD. The effect of t is also significant, but to a lower extent, while T has a low impact on the electrochemical degradation of tannery wastewater.

The current density is the key parameter for the degradation of wastewater as it regulates the generation of hydroxyl radicals ($^{\bullet}$OH) on the electrode surface [39]. Increasing j enhances the production of electrons, which facilitates the generation of physisorbed and chemisorbed radicals on the surface of the anode [26]. This increase causes the acceleration of the degradation process.

EO of organics begins with the formation of adsorbed $^{\bullet}$OH radicals from water discharge reactions at the surface of the anode (Eq. (8)).

$$\frac{\text{Ti}}{\text{Pt}} + \text{H}_2\text{O} \rightarrow \frac{\text{Ti}}{\text{Pt}}\left(^{\bullet}\text{OH}\right) + \text{H}^+ + e^- \tag{8}$$

Reactivity of electrochemically generated hydroxyl radicals depends upon the nature of the electrode materials. Ti/Pt anode is an active anode and strongly interacts with $^\bullet$OH radicals to form the higher metal oxides (Ti/Pt (O)) (Eq. (9)).

$$\frac{\mathrm{Ti}}{\mathrm{Pt}}\left(^\bullet\mathrm{OH}\right) \rightarrow \frac{\mathrm{Ti}}{\mathrm{Pt}}\left(\mathrm{O}\right) + \mathrm{H}^+ + \mathrm{e}^- \tag{9}$$

In this case, the (Ti/Pt(O)/Ti/Pt($^\bullet$OH)) redox couple acts as a mediator during the electrochemical degradation (Eq. (10)), thus allowing selective oxidation of organics present in wastewater. However, a competitive side reaction of oxygen evolution takes place due to the chemical decomposition of the higher oxide (Eq. (11)) [40].

$$\frac{\mathrm{Ti}}{\mathrm{Pt}}\left(\mathrm{O}\right) + \mathrm{R} \rightarrow \frac{\mathrm{Ti}}{\mathrm{Pt}} + \mathrm{RO} \tag{10}$$

$$\frac{\mathrm{Ti}}{\mathrm{Pt}}\left(\mathrm{O}\right) \rightarrow \frac{\mathrm{Ti}}{\mathrm{Pt}} + \frac{1}{2}\mathrm{O}_2 \tag{11}$$

From Fig. 4a, it can be seen that current density and electrolysis time affect positively the degradation of wastewater. Thus, the COD removal rate increases significantly with an increase of current density from 5.4 to 19.5 mA/cm^2. Also, it increases with increasing electrolysis time from 1.32 to 4.68 h at all range of *j* values. However, the removal efficiency was marginal toward higher *j* and Fig. 4c shows that the SEC increases with an increase of both current density and electrolysis time. This fact can be explained by the accumulation of by-products that are quite stable against further attack at the Ti/Pt anode during the degradation process of wastewater [41]. Moreover, the passivation of the anode surface by the growth of poisoned adherent layer during the electrolysis reduces its efficiency for further oxidation [8]. In addition, the concomitant rise in the rate of parasitic anodic oxygen evolution reaction could also contribute and negatively affect the degradation efficiency [15].

Temperature also affects the treatment efficiency with EO process but to a lower extent. Fig. 4b shows that increasing temperature had a negative influence on the electrochemical degradation. It is worthy to mention that tannery wastewater contains a large variety of inorganic ions that can result in

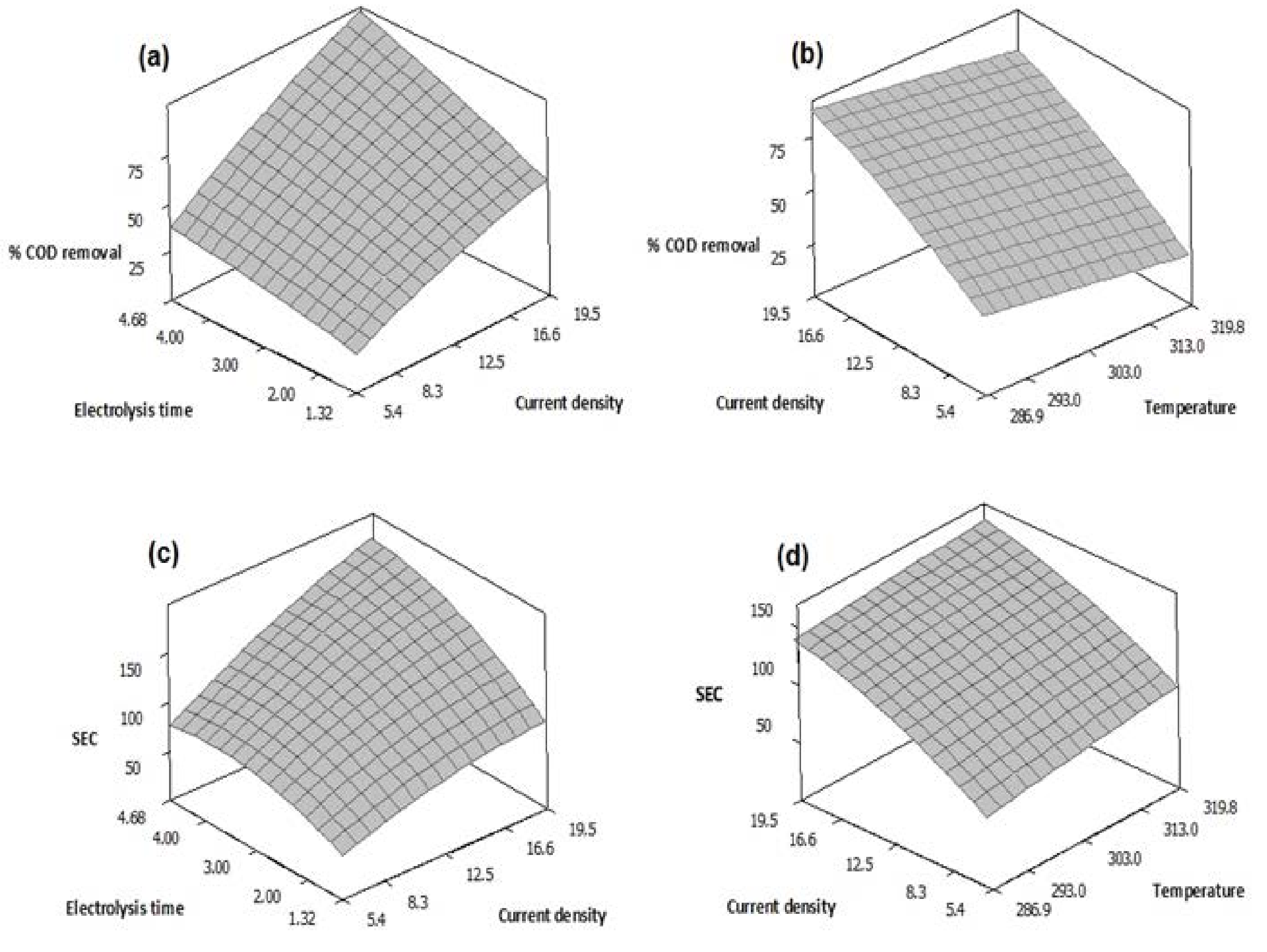

Fig. 4. Response surface for both removal of COD and specific energy consumption during EO treatment of wastewater, (a) electrolysis time and current density, (b) current density and temperature, (c) electrolysis time and current density, and (d) current density and temperature.

the production of strong mediated oxidants, such as active chlorine (in the form of Cl_2, HOCl or OCl^-). Also, when active anodes are used, the Cl^- mediated oxidation raised the performance of the electrochemical process. In fact, organic pollutants can be removed by generating in situ active chlorine species that convert them from hazardous compounds to less harmful products. Immediately afterward, the discharge of chlorine gas (Eq. (12)), provided anodically by chloride naturally present or added to the solution, reactions of hydrolysis (Eq. (13)) and ionization (Eq. (14)) take place.

$$2Cl^- \rightarrow Cl_2 + 2e^- \tag{12}$$

$$Cl_2 + H_2O \rightarrow HOCl + H^+ + Cl^- \tag{13}$$

$$HOCl \rightarrow H^+ + OCl^- \tag{14}$$

The enhancement of effluent degradation efficiency with a decrease in temperature could be attributed to several factors. Considering the mediated mechanism, the temperature has an effect on the competition between water and chloride oxidation. The oxygen evolution rate reduces while decreasing the temperature of the solution, leading to a further enhancement in the active chlorine yield [42]. Furthermore, the conversion of a part of Cl^- in solution to $Cl_2(g)$ at 40°C can negatively affect the indirect oxidation process [43]. However, as shown in Fig. 4d temperature did not have a significant influence on the SEC as the value of SEC changes very slightly with rising *T*.

Numerical optimization was employed to determine the optimum values of the process variables for maximum COD removal efficiency and minimum SEC. Based on RSM and the desirability functions, optimum conditions for the treatment of tannery wastewater were found to be $t = 2.11$ h, $j = 18.70$ mA/cm^2 and $T = 286.18$ K. These results were predicted based on desirability function of 0.967.

3.4. Evolution of released inorganic ions

Electro-generated $^{\bullet}OH$ and active chlorine species act as strong oxidants and completely mineralize the organic contaminants present in wastewater, thus releasing the inorganic ions species and nitrogenated ions, such as nitrate (NO_3^-) and nitrite (NO_2^-). Fig. 5 presents the evolution of nitrate and nitrite ions concentrations, accumulated during the treatment of wastewater by the EO process. As can be observed, the nitrate concentration increased progressively with treatment time, while the nitrite concentration increased slightly and then decreased. This demonstrates that further oxidation reactions by electrogenerated oxidants lead to more formation of NO_3^- by the oxidation of NO_2^-.

3.5. Changes of turbidity, pH and conductivity with treatment time

Turbidity and COD measurements were carried out to follow the degradation of the effluent (Fig. 6a). Both turbidity and COD removal increased with electrolysis. However, 73% of turbidity removal was achieved within 3 h of electrolysis time while COD removal did not reach more than 54%, meaning the less efficient removal of COD than that of turbidity. Similar observations were made by Li et al. [44] for EO of biologically treated citric acid wastewater using a Ti/RuO_2–IrO_2 anode. They found that the COD removal rate

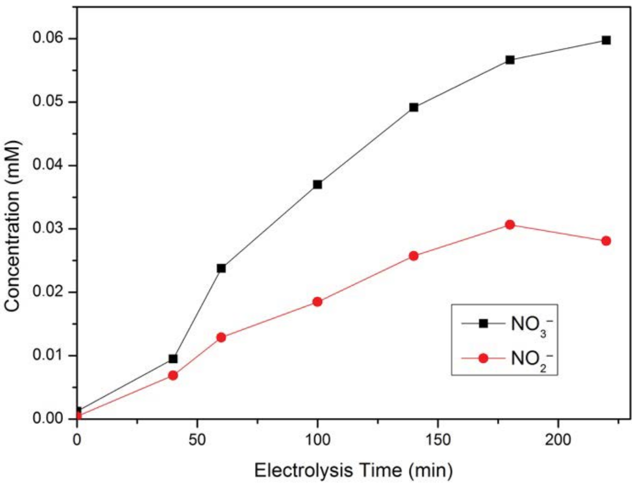

Fig. 5. Concentration evolution of inorganic ions formed during the EO treatment of wastewater.

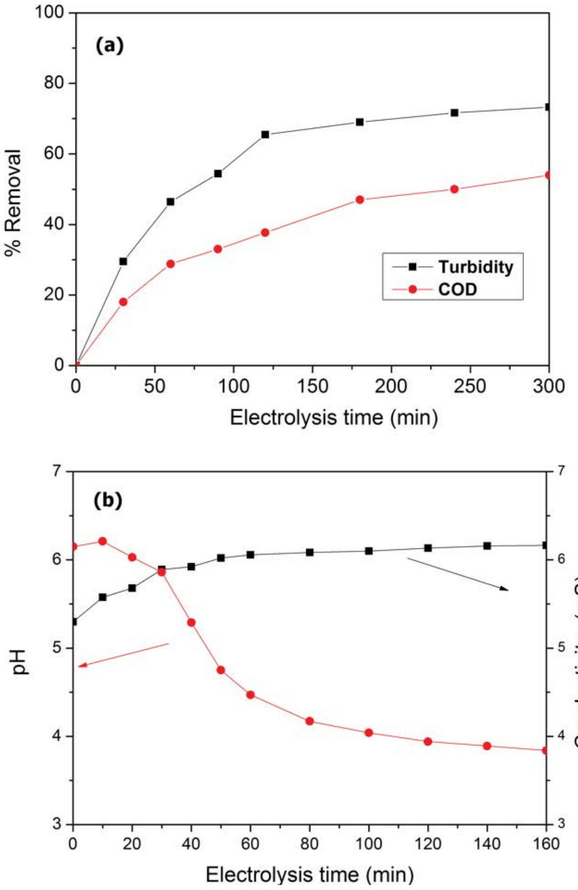

Fig. 6. (a) Turbidity and COD removal and (b) pH conductivity changes during the EO process ($j = 8.3$ mA cm^{-2}; $T = 303$ K).

(0.009 min^{-1}) was lower than that of turbidity (0.017 min^{-1}). The faster removal of turbidity and the partial mineralization of COD could be attributed to the degradation of organic compounds by the destruction of chromophoric groups or by a break-down of macromolecular chains. The limited increase of turbidity removal was also related to the presence of inorganic material suspended in the tannery effluent.

Furthermore, the pH and conductivity variation of tannery wastewater were also recorded with the electrolysis time, as shown in Fig. 6b. The pH decreased gradually from an initial value of 6.15 to a value of 3.83 after 160 min of electrolysis. This significant decrease in pH was mainly due to an abundant generation of H$^+$ through hypochlorous acid generation as illustrated in Eq. (14) and other parasitic side reactions such as oxygen evolution reaction (Eq. (15)) [45,46].

$$2H_2O \rightarrow O_2 + 4H^+ + 4e^- \tag{15}$$

Previous studies in the electrochemical treatment of wastewater also reported a similar trend [47,48]. Authors supposed that pH decreases were attributed to the production of carboxylic acids as intermediate products. These assumptions are confirmed with the changes in COD removal reported in Fig. 6a.

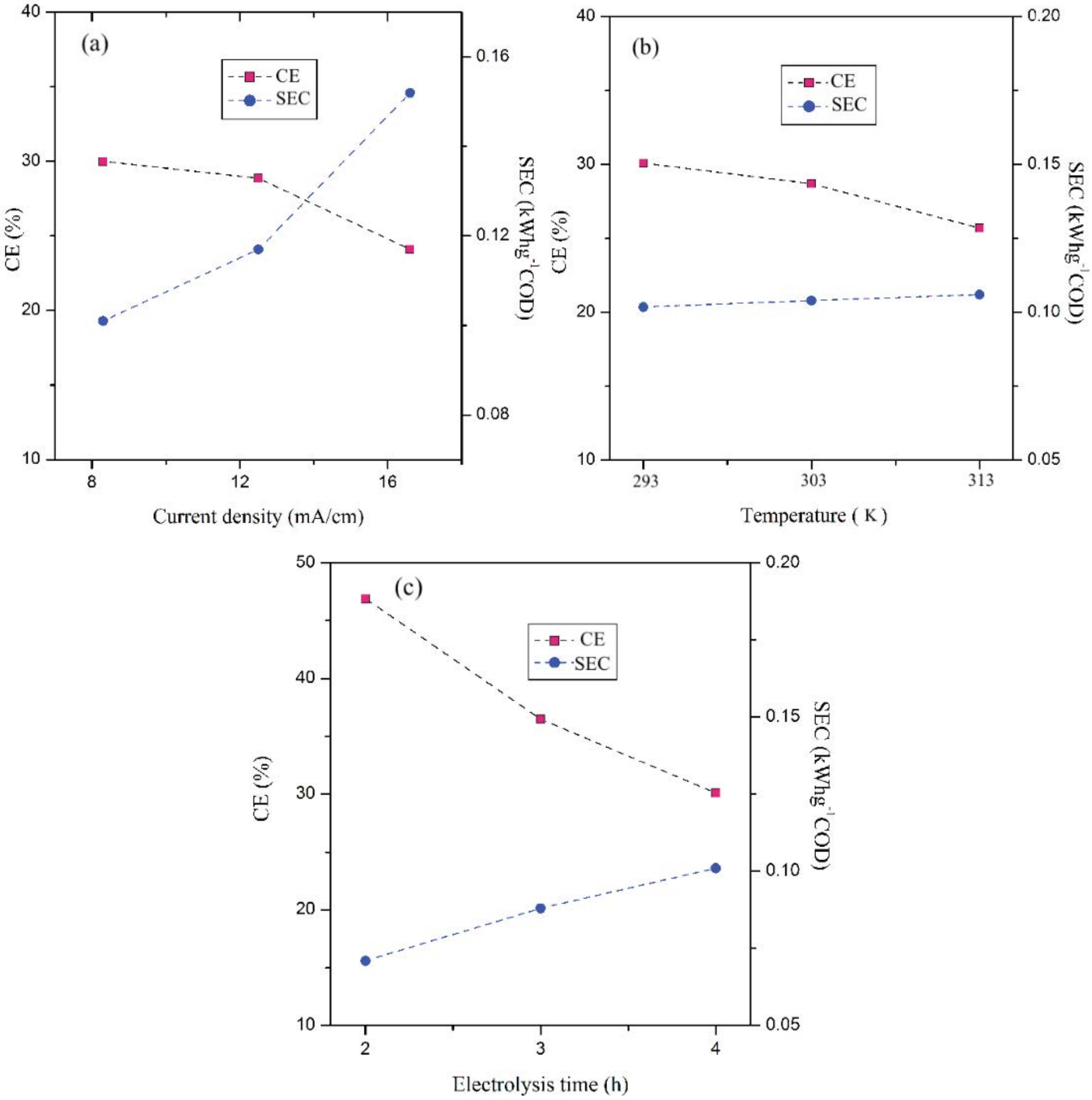

Fig. 7. Current efficiency and energy consumption as function of (a) current density, (b) temperature and (c) electrolysis time.

Table 5
Degradation of tannery wastewater by EO using different anode materials

Parameter/initial concentration (mg L^{-1})	Electrode material	Current density (mA/cm^2)	Volume (mL)	Time (h)	Removal %	EC %	SEC kWh/kg	References
COD 623	Ti/Pt	18.7	5,500	2.11	81.2	41.1	93.85	This study
COD 1,774	Ti/Pt-Ir	30	640	0.5	10.9	20.6	111	[50]
COD 352	Graphite	12	2,000	2	59.73	4.0	–	[51]
TOC 1,005	$Ti/Ir_0.15Ru_0.15Sn_0.70O_2$	20	50	3	14.3	38.5	–	[52]
COD 2,417	$Ti/SnO_2/PdO_2/RuO_2$	20	1,030	1	77.3	70.2	–	[2]
COD 1,150	BDD	25	1,200	2	56.3	–	–	[53]

The conductivity values slightly increased by 40 min up to 6.05 mS from 5.28 mS, and then fluctuated between 6.08 and 6.16 mS.

3.6. Current efficiency and energy consumptions

Fig. 7 shows the variation of current efficiency and energy consumption as a function of different operating conditions (electrolysis time, current density and temperature). As illustrated in Fig. 7a, the CE value decreased slightly when increasing current density from 8.3 to 12.5 mA cm^{-2}, but decreased sharply at higher current density (16.6 mA cm^{-2}). In contrast, increases in current density lead to higher energy consumption. This behavior was observed in previous studies [6] and is probably due to the undesired side reactions, for example, rise in oxygen evolution at higher current densities. The variation of current efficiency and energy consumption with temperature is presented in Fig. 7b. As concluded earlier, the temperature had a marginal effect on current efficiency. CE value increased slightly from 25.8% to 28.7% when the temperature decreased from 40°C to 30°C, then it increased more slightly at a temperature of 20°C. However, the energy consumption was independent of the temperature value. Finally, from the results shown in Fig. 7c, it is concluded that the electrochemical oxidation at an extended electrolysis time is disadvantageous. Decreases in electrolysis time increased the anode efficiency and decreased energy consumption.

On the basis of these results and at the optimum EO conditions of leather dyeing wastewater treatment, COD removal, CE and SEC values were found to be 81,2%, 41,1% and 93,85 kWh per kg of COD removed, respectively. These values were compared with relevant results obtained with the EO process for tannery wastewater treatment reported in Table 5. As can be observed, the most investigated type of electrode for tannery wastewater treatment was a DSA coating titanium anode, due to their excellent electrocatalytic properties, especially for chlorine generation. However, these anodes have low current efficiency, since they favor side reactions [49]. The BDD electrode exhibited a good result, but it has a major drawback of high cost. Good performance was also obtained with metal oxide electrode.

4. Conclusion

In the present study, the electrochemical oxidation of real dyeing leather wastewater was studied using Ti/Pt anode. Full factorial CCD methodology was used to determine the optimal condition for effluent treatment in terms of cost-effectiveness. The influence of the operating condition on the current efficiency was also assessed. The COD removal efficiency was mainly affected by applied current density. Energy consumption was largely affected by electrolysis time and current density, but a modest influence of the temperature on energy requirements was observed. Under the optimal condition, it was possible to achieve 81.2% of COD removal with a significant reduction in the treatment time and energy consumption (93.85 kWh). The high efficiency obtained with acceptable energy requirements and short electrolysis time indicates the feasibility of EO as an alternative treatment of real leather dyeing wastewater.

These promising results could encourage full-scale implementation of the EO process using electrocatalytic electrodes as a treatment for actual effluents. However, the probable formation of toxic chlorinated compounds during EO especially in presence of high concentrated chlorides can be considered as a serious drawback of this system that has to be carefully studied before the introduction of the process at industrial scale. In addition, as in the case of all the electrochemical methods, the high operational cost for electricity represents an obstacle for large-scale application. Combining biological treatment with EO and the use of renewable power would be suitable alternatives to overcome this drawback and make this process feasible on an industrial scale.

References

[1] S.G. Schrank, W. Gebhardt, H.J. José, R.F. Moreira, H.F. Schröder, Ozone treatment of tannery wastewater monitored by conventional and substance specific wastewater analyses, Ozone Sci. Eng., 39 (2016) 159–187.

[2] J.H. Naumczyk, M.A. Kucharska, Electrochemical treatment of tannery wastewater—raw, coagulated, and pretreated by AOPs, J. Environ. Sci. Health, Part A, 52 (2017) 649–664.

[3] F.M.M. Paschoal, M.A. Anderson, M.V.B. Zanoni, Simultaneous removal of chromium and leather dye from simulated tannery effluent by photoelectrochemistry, J. Hazard. Mater., 166 (2009) 531–537.

[4] B. Mella, B.S.D.C. Barcellos, D.E. da Silva Costa, M. Gutterres, Treatment of leather dyeing wastewater with associated process of coagulation-flocculation/adsorption/ozonation, Ozone Sci. Eng., 40 (2017) 133–140.

[5] J.S. Piccin, C.S. Gomes, B. Mella, M. Gutterres, Color removal from real leather dyeing effluent using tannery waste as an adsorbent, J. Environ. Chem. Eng., 4 (2016) 1061–1067.

[6] A.S. Fajardo, R.C. Martins, D.R. Silva, R.M. Quinta-Ferreira, C.A. Martínez-Huitle, Electrochemical abatement of amaranth dye solutions using individual or an assembling of flow cells

with Ti/Pt and Ti/Pt-SnSb anodes, Sep. Purif. Technol., 179 (2017) 194–203.

[7] Y. Xue, S. Zheng, H. Du, Y. Zhang, W. Jin, Cr(III)-induced electrochemical advanced oxidation processes for the V_2O_3 dissolution in alkaline media, Chem. Eng. J., 307 (2016) 518–525.

[8] C.A. Martínez-Huitle, M.A. Rodrigo, I. Sirés, O. Scialdone, Single and coupled electrochemical processes and reactors for the abatement of organic water pollutants: a critical review, Chem. Rev., 115 (2015) 13362–13407.

[9] G. Azarian, M. Miri, D. Nematollahi, Combined electrocoagulation/electrooxidation process for the COD removal and recovery of tannery industry wastewater, Environ. Prog. Sustain. Energy, 37 (2018) 637–644.

[10] X. Tu, S. Xiao, Y. Song, D. Zhang, Treatment of simulated berberine wastewater by electrochemical process with Pt/Ti anode, Environ. Earth Sci., 73 (2015) 4957–4966.

[11] A.N.S. Rao, V.T. Venkatarangaiah, Metal oxide-coated anodes in wastewater treatment, Environ. Sci. Pollut. Res., 21 (2014) 3197–3217.

[12] J.L. da Silva Duarte, A.M.S. Solano, M.L. Arguelho, J. Tonholo, C.A. Martínez-Huitle, C.L.D.P. de Silva, Evaluation of treatment of effluents contaminated with rifampicin by Fenton, electrochemical and associated processes, J. Water. Process Eng., 22 (2018) 250–257.

[13] S. Cotillas, J. Llanos, P. Cañizares, D. Clematis, G. Cerisola, M. A. Rodrigo, M. Panizza, Removal of Procion Red MX-5B dye from wastewater by conductive-diamond electrochemical oxidation, Electrochim. Acta, 263 (2018) 1–7.

[14] L. Labiadh, A. Barbucci, M.P. Carpanese, A. Gadri, S. Ammar, M. Panizza, Comparative depollution of Methyl Orange aqueous solutions by electrochemical incineration using $TiRuSnO_2$, BDD and PbO_2 as high oxidation power anodes, J. Electroanal. Chem., 766 (2016) 94–99.

[15] E. Isarain-Chávez, M.D. Baró, E. Rossinyol, U. Morales-Ortiz, J. Sort, E. Brillas, E. Pellicer, Comparative electrochemical oxidation of methyl orange azo dye using Ti/Ir-Pb, Ti/Ir-Sn, Ti/Ru-Pb, Ti/Pt-Pd and Ti/RuO_2 anodes, Electrochim. Acta., 244 (2017) 199–208.

[16] P. Kaur, J.P. Kushwaha, V.K. Sangal, Evaluation and disposability study of actual textile wastewater treatment by electro-oxidation method using Ti/RuO_2 anode, Process Saf. Environ. Prot., 111 (2017) 13–22.

[17] A.G. Vlyssides, M. Loizidou, P.K. Karlis, A.A. Zorpas, D. Papaioannou, Electrochemical oxidation of a textile dye wastewater using a Pt/Ti electrode, J. Hazard. Mater., 70 (1999) 41–52.

[18] W.L. Chou, C.T. Wang, C.P. Chang, M.H. Chung, Y.M. Kuo, Removal of color and COD from dyeing wastewater by paired electrochemical oxidation, Fresenius Environ. Bull., 20 (2011) 78–85.

[19] X. Zhu, J. Ni, J. Wei, X. Xing, H. Li, Destination of organic pollutants during electrochemical oxidation of biologically-pretreated dye wastewater using boron-doped diamond anode, J. Hazard. Mater., 189 (2011) 127–133.

[20] S.S. Vaghela, A.D. Jethva, B.B. Mehta, S.P. Dave, S. Adimurthy, G. Ramachandraiah, Laboratory studies of electrochemical treatment of industrial azo dye effluent, Environ. Sci. Technol., 39 (2005) 2848–2855.

[21] C.T. Wang, W.L. Chou, Y.M. Kuo, F.L. Chang, Paired removal of color and COD from textile dyeing wastewater by simultaneous anodic and indirect cathodic oxidation, J. Hazard. Mater., 169 (2009) 16–22.

[22] J.M. Aquino, R.C. Rocha-Filho, L.A. Ruotolo, N. Bocchi, S.R. Biaggio, Electrochemical degradation of a real textile wastewater using β-PbO_2 and DSA® anodes, Chem. Eng. J., 251 (2014) 138–145.

[23] APHA-AWWA-WPCF, Standard Methods for the Examination of Water and Wastewater, 22nd ed., Washington, 2012.

[24] APHA-AWWA-WEF, Standard Methods for the Examination of Water and Wastewater, 19th ed., Washington, 1995.

[25] F. Torrades, S. Saiz, J.A. García-Hortal, Using central composite experimental design to optimize the degradation of black liquor by Fenton reagent, Desalination, 268 (2011) 97–102.

[26] A. Goyal, V.C. Srivastava, J.P. Kushwaha, Treatment of highly acidic wastewater containing high energetic compounds using dimensionally stable anode, Chem. Eng. J., 325 (2017) 289–299.

[27] S. Sadaf, H.N. Bhatti, Batch and fixed bed column studies for the removal of Indosol Yellow BG dye by peanut husk, J. Taiwan Inst. Chem. Eng., 45 (2014) 541–553.

[28] P. Kariyajjanavar, J. Narayana, Y.A. Nayaka, Degradation of textile dye C.I. Vat Black 27 by electrochemical method by using carbon electrodes, J. Environ. Chem. Eng., 1 (2013) 975–980

[29] V. Subbaramaiah, V.C. Srivastava, I.D. Mall, Catalytic oxidation of nitrobenzene by copper loaded activated carbon, Sep. Purif. Technol., 125 (2014) 284–290.

[30] G.K. Parshetti, A.A. Telke, D.C. Kalyani, S.P. Govindwar, Decolorization and detoxification of sulfonated azo dye methyl orange by Kocuria rosea MTCC 1532, J. Hazard. Mater., 176 (2010) 503–509.

[31] J. Coates, In: R.A. Meyers, Ed., Encyclopedia of Analytical Chemistry, John Wiley & Sons Ltd, Chichester 2000, pp. 10815–10837.

[32] B. Yadav, V.C. Srivastava, Catalytic peroxidation of recalcitrant quinoline by ceria impregnated granular activated carbon, Clean Technol. Environ. Policy, 19 (2016) 1547–1555.

[33] V. Singh, A.K. Sharma, D.N. Tripathi, R. Sanghi, Poly (methylmethacrylate) grafted chitosan: an efficient adsorbent for anionic azo dyes, J. Hazard. Mater., 161 (2009) 955–966.

[34] S. Raghu, C.W. Lee, S. Chellammal, S. Palanichamy, C.A. Basha, Evaluation of electrochemical oxidation techniques for degradation of dye effluents-a comparative approach, J. Hazard. Mater., 171 (2009) 748–754.

[35] M. Amini, H. Younesi, N. Bahramifar, A.A.Z. Lorestani, F. Ghorbani, A. Daneshi, M. Sharifzadeh, Application of response surface methodology for optimization of lead biosorption in an aqueous solution by Aspergillus niger, J. Hazard. Mater., 154 (2008) 694–702.

[36] J. Wu, H. Zhang, N. Oturan, Y. Wang, L. Chen, M.A. Oturan, Application of response surface methodology to the removal of the antibiotic tetracycline by electrochemical process using carbon-felt cathode and DSA (Ti/RuO_2–IrO_2) anode, Chemosphere, 87 (2012) 614–620.

[37] M. Moradi, F. Ghanbari, E.M. Tabrizi, Removal of Acid Yellow 36 using Box-Behnken designed photoelectro-Fenton: a study on removal mechanisms, Toxicol. Environ. Chem., 97 (2015) 700–709.

[38] M. Moradi, F. Ghanbari, M. Manshouri, K.A. Angali, Photocatalytic degradation of azo dye using nano-ZrO_2/UV/persulfate: response surface modeling and optimization, Korean J. Chem. Eng., 33 (2016) 539–546.

[39] D. Li, J. Tang, X. Zhou, J. Li, X. Sun, J. Shen, L. Wang, W. Han, Electrochemical degradation of pyridine by Ti/SnO_2–Sb tubular porous electrode, Chemosphere, 149 (2016) 49–56.

[40] M. Panizza, In: Electrochemistry for the Environment, Springer, New York, 2010, pp. 25–54.

[41] A.D. Hiwarkar, S. Singh, V.C. Srivastava, I.D. Mall, Mineralization of pyrrole, a recalcitrant heterocyclic compound, by electrochemical method: multi-response optimization and degradation mechanism, J. Environ. Manage., 198 (2017) 144–152.

[42] F. Bonfatti, S. Ferro, F. Lavezzo, M. Malacarne, G. Lodi, A. De Battisti, Electrochemical incineration of glucose as a model organic substrate, II. Role of Active Chlorine Mediation, J. Electrochem. Soc., 147 (2000) 592–596.

[43] F.L.G. de Menezes, A.J.C. da Silva, C.A. Martínez-Huitle, C.L.P.S. Zanta, J.J.F. Alves, S.S.L. Castro, Electrochemical treatment of shrimp farming effluent: role of electrocatalytic material, Environ. Sci. Pollut. Res., 24 (2017) 6061–6070.

[44] X. Li, C. Wang, Y. Qian, Y. Wang, L. Zhang, Simultaneous removal of chemical oxygen demand, turbidity and hardness from biologically treated citric acid wastewater by electrochemical oxidation for reuse, Sep. Purif. Technol., 107 (2013) 281–288.

[45] J. Zou, X. Peng, M. Li, Y. Xiong, B. Wang, F. Dong, B. Wang, Electrochemical oxidation of COD from real textile wastewaters: kinetic study and energy consumption, Chemosphere, 171 (2017) 332–338.

[46] B.K. Körbahti, N. Aktaş, A. Tanyolac, Optimization of electrochemical treatment of industrial paint wastewater with response surface methodology, J. Hazard. Mater., 148 (2007) 83–90.

[47] S.K. Johnson, L.L. Houk, J. Feng, R.S. Houk, D.C. Johnson, Electrochemical incineration of 4-chlorophenol and the identification of products and intermediates by mass spectrometry, Environ. Sci. Technol., 33 (1999) 2638–2644.

[48] A.M.S. Solano, C.K.C. de Araújo, J.V. de Melo, J.M. Peralta-Hernandez, D.R. da Silva, C.A. Martínez-Huitle, Decontamination of real textile industrial effluent by strong oxidant species electrogenerated on diamond electrode: viability and disadvantages of this electrochemical technology, Appl. Catal. B Environ., 130 (2013) 112–120.

[49] P. Mandal, B.K. Dubey, A.K. Gupta, Review on landfill leachate treatment by electrochemical oxidation: drawbacks, challenges and future scope, Waste Manage., 69 (2017) 250–273.

[50] L. Szpyrkowicz, J. Naumczyk, F. Zilio-Grandi, Electrochemical treatment of tannery wastewater using TiPt and Ti/Pt/Ir electrodes, Water Res., 29 (1995) 517–524.

[51] S. Sundarapandiyan, R. Chandrasekar, B. Ramanaiah, S. Krishnan, P. Saravanan, Electrochemical oxidation and reuse of tannery saline wastewater, J. Hazard. Mater., 180 (2010) 197–203.

[52] C.R. Coast, C.M.R. Botta, E.L.G. Espindola, P. Olivi, Electrochemical treatment of tannery wastewater using DSA® electrodes, J. Hazard. Mater., 153 (2008) 616–627.

[53] W.H. Liu, C.G. Zhang, P.F. Gao, H. Liu, Y.Q. Song, J.F. Yang, Advanced treatment of tannery wastewater using the combination of UASB, SBR, electrochemical oxidation and BAF, J. Chem. Technol. Biotechnol., 92 (2017) 588–597.